DE GRUYTER OPEN

Structural and optical characteristics of SnS thin film prepared by SILAR

A. MUKHERJEE*, P. MITRA

Dept. of Physics, The University of Burdwan, Golapbag, Burdwan-713104, India

SnS thin films were grown on glass substrates by a simple route named successive ion layer adsorption and reaction (SILAR) method. The films were prepared using tin chloride as tin (Sn) source and ammonium sulfide as sulphur (S) source. The structural, optical and morphological study was done using XRD, FESEM, FT-IR and UV-Vis spectrophotometer. XRD measurement confirmed the presence of orthorhombic phase. Particle size estimated from XRD was about 45 nm which fitted well with the FESEM measurement. The value of band gap was about 1.63 eV indicating that SnS can be used as an important material for thin film solar cells. The surface morphology showed a smooth, homogenous film over the substrate. Characteristic stretching vibration mode of SnS was observed in the absorption band of FT-IR spectrum. The electrical activation energy was about 0.306 eV.

Keywords: *SnS; SILAR; thin films; FESEM; FT-IR*

1. Introduction

In recent times semiconducting metal chalcogenide thin films have attracted a huge attention for their potential application in solid state devices, such as photovoltaic, photoelectrochemical (PEC), photoconductive cells, solar cells, polarizers, sensors etc. [1]. Among different semiconducting metal chalcogenides, tin sulphide has drawn great interest due to its large optical absorption coefficient with high photoelectric conversion efficiency [2]. SnS belongs to IV – VI semiconductors formed by Sn and S elements which are abundant in nature, cheap and non-toxic. SnS is found in zinc blende (a = 0.5845 nm) as well as orthorhombic (a = 0.385 nm, b = 1.142 nm and c = 0.438 nm) and herzenbergite crystal structures [3]. Generally, the material shows a p-type electrical conductivity and its electrical conductivity can be controlled by different dopants. The reported optical band-gap of SnS films varies between 1.1 and 2.1 eV depending on their fabrication process [4, 5]. Despite these attractive properties, solar cells based on SnS absorbers have not achieved conversion efficiency higher than 1.3 % [6], while theoretically such cells should be able to reach 24 % efficiency [7]. This poor performance may be due to defects and/or impurities present in SnS layers that result from the preparation methods or chemicals used to make such films [8]. The films can be fabricated using different techniques, such as spray pyrolysis, electrodeposition, chemical bath deposition, vacuum evaporation, SILAR, etc. Among all of them, SILAR is the simplest, inexpensive and low time consuming method compared to the others [9]. SILAR can be used for large area thin film deposition and the thickness can be controlled by the number of dipping. In mid-1980's Nicolau first introduced SILAR method [10]. SILAR is a new version of CBD and is often called modified CBD. In our work, we report on structural, morphological, electrical and optical properties of SnS thin film prepared by SILAR. We have tried a new route to fabricate sodium free SnS sample. A uniform, adherent brown colored film was obtained on the glass substrate.

2. Experimental

Tin sulfide (SnS) thin film was synthesized by dipping a pre-cleaned glass substrate alternately in

---

*E-mail: ayanmukherjee88@gmail.com

stannous chloride $SnCl_2 \cdot 2H_2O$ solution taken as a cationic precursor (which was kept at ∼70 °C) and 2 vol. % ammonium sulfide $[(NH_4)_2S]$ solution at room temperature taken as anionic precursor. Between every immersion in cationic and anionic precursors, the film was rinsed with distilled water. The concentration of cationic precursor was 0.025 M. The tin chloride bath was prepared by adding tin chloride in distilled water. Similarly, ammonium sulfide solution (40 to 48 wt.%, Sigma Aldrich) was prepared by adding 2 cm^3 ammonium sulfide into 100 cm^3 distilled water. Concentrations of the reacting baths were optimized in order to obtain good quality adherent films. As stannous chloride solution did not dissolve completely, a drop of acetic acid was added to get a clear transparent solution. The solution of ammonium sulphide was stable and no stirring was required. Alternate dipping of the substrate in cationic and anionic precursors led to the formation of SnS thin film. The film deposition process consisted of the following steps: (i) dipping of the substrate in the stannous chloride solution kept at 70 °C, which carried a thin layer of tin ion adhering to the surface of the substrate and (ii) introduction of the substrate into ammonium sulphide bath kept at room temperature. The reaction between tin ions and sulphur ions led to the formation of SnS, thus, a layer of SnS was formed. Consequently, one complete dipping cycle included dipping the substrate into stannous chloride bath, its withdrawal from the bath followed by dipping into the distilled water, then dipping into ammonium sulphide bath and finally dipping in distilled water. The dipping time in each bath was about 5 seconds. The number of dipping cycles was fixed to get a film of thickness about 600 nm.

X-ray diffraction (XRD) measurements were carried out employing a Bruker D8 advanced diffractometer for structural characterization of the synthesized film. The phase identification and crystalline properties of the film were studied from the XRD pattern with CuKα radiation ($\lambda = 1.5418$ Å) and compared with standard JCPDS files. Field emission scanning electron microscopy (FESEM) was used to measure the particle size. The same instrument was used for energy dispersive X-ray

(EDX) analysis. The optical measurements were performed using a Schimatzu UV-Vis spectrophotometer (model UV-1800). Absorption spectrum was recorded with the spectrophotometer using a similar glass as reference, hence, the absorption spectra of the film were obtained. The band gap of the film was calculated from the absorption edge of the spectrum. The thin film sample was electroded with silver (Ag) conducting paste on a single side, maintaining equal gap for all samples. Copper connecting wires were used for resistance measurement using a Keithley 6514DMM. The conductance was calculated depending on temperature variation.

3.   Results and discussion

X-ray diffraction (XRD) pattern of SnS thin film is shown in Fig. 1. It is in good agreement with the standard JCPDS Card No. 39-0354. First three prominent peaks are observed at angular positions 2θ = 21.95°, 26.48° and 30.65°, clearly indicating the presence of orthorhombic phase. The corresponding peak positions in JCPDS are 22.01°, 26.09° and 30.473°. All the other peaks with smaller intensity are in agreement with JCPDS file. These diffraction peaks correspond to (1 1 0), (1 2 0) and (1 0 1) planes, respectively (JCPDS Card No. 39-0354).

The pattern fitted using Rietveld refinement software is shown in Fig. 2. The interplanar spacings of the planes are 4.04 Å, 3.36 Å and 2.92 Å and the corresponding JCPDF values are 4.035 Å, 3.423 Å and 2.931 Å, respectively. The lattice parameters were calculated by Rietveld refinement of XRD data using MAUD software [11]. The obtained values of lattice parameters are a = 4.074±0.0082 Å, b = 4.153±0.0054 Å and c = 11.639±0.0084 Å. The goodness of fit (GOF) of the Rietveld refinement is 1.068 indicating good quality of fitting. The refinement also gives the value of Sn–S bond length = 2.6763 Å and average particle size of ∼45 nm. The values of particle size obtained from the Rietveld refinement for (1 1 0), (1 2 0) and (0 2 1) planes were 43.2 nm, 46.7 nm and 45.2 nm, respectively.
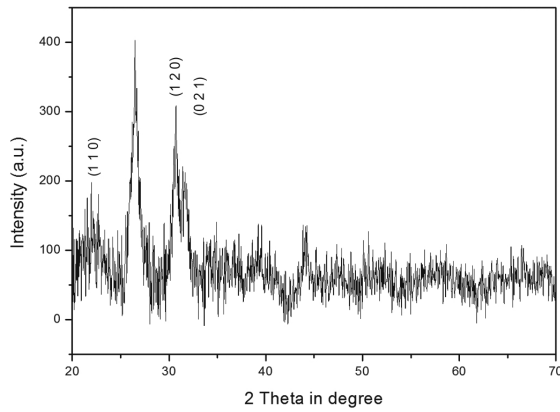
Fig. 1. XRD pattern of SnS thin film.

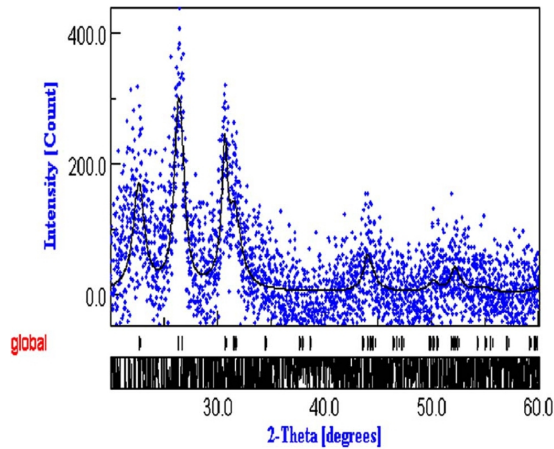Fig. 2. XRD pattern of SnS thin film (experimental (dotted) and fitted (continuous)).

Fig. 3. EDX spectrum of SnS film.

Fig. 4. FESEM image of SnS film.

EDX spectrum of SnS film is shown in Fig. 3. The micrograph shows the presence of Sn and S elements and absence of sodium impurity. Fig. 4 shows an FESEM image of the film. The image shows uniformly distributed grains of nanometer size all over the surface. The average size of the grains calculated using ImageJ software [12] is about 46.5 nm which matches well with X-ray value of ∼45 nm. The observed surface properties have a strong effect on the optical properties of the thin film, such as transmission, absorption and reflection [3].

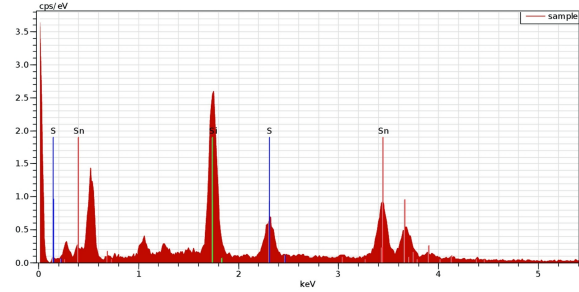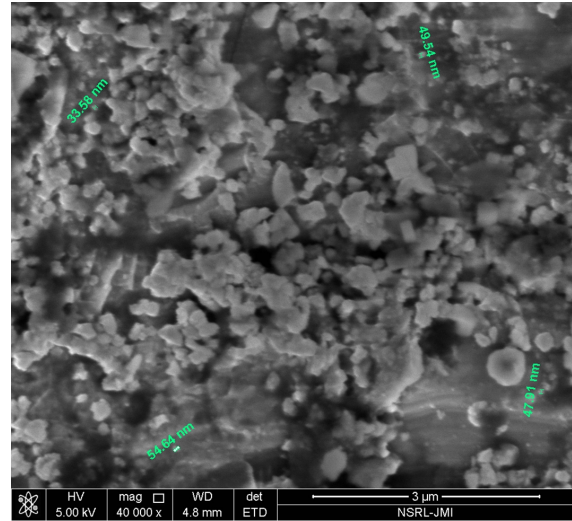The absorption spectra of the SnS thin film were obtained between 200 nm and 900 nm at room temperature using UV-Vis spectrophotometer. The band gap was evaluated using the absorption coefficient α:

$$\alpha = 2.303 \frac{A}{t} \tag{1}$$

where A and t are film absorbance and thickness, respectively. Band gap is usually evaluated using Tauc formula [13] based on a graph of $(\alpha h \nu)^2$ vs. $h\nu$. The linear region of this plot is extrapolated to the intersect with the x axis at y = 0. The intersecting point gives the optical bandgap (ε_g):

$$(\alpha h \nu)^2 = K (h \nu - \varepsilon_g) \tag{2}$$

where K is the proportionality constant. The obtained band gap energy obtained from the Tauc plot is ∼1.6 eV as shown in Fig. 5. The transmission spectrum is shown in Fig. 6, where the percentage transmission against wavelength is plotted. The value of the obtained band gap is on

the higher side of the bulk value (∼1.43 eV) for bulk tin sulphide [19]. The difference in band gap may be attributed to quantum confinement effect arising from lowering of particle size. It has also been reported that the optical band gap varies with tin-to-sulphur ratio in the structure leading to the change in energy band structure and also the density of states (DOS) of valence band and conduction band [19]. Thus, compositional stoichiometry may also contribute to enhanced band gap.
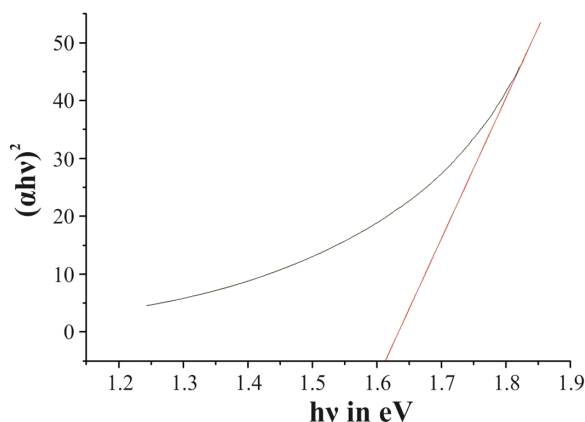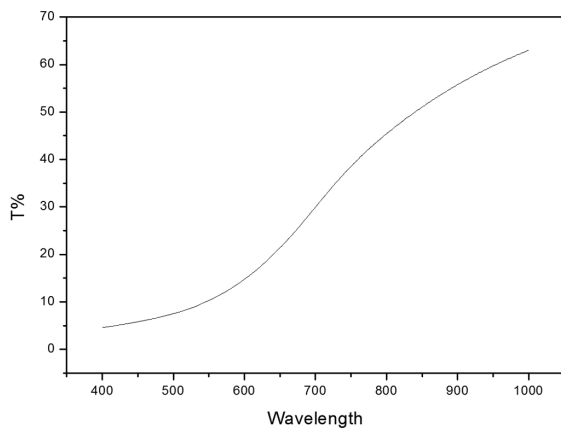

Fig. 5. Tauc plot of SnS.

Fig. 6. Transmission spectra of SnS film.

To study the electrical conductivity of the SnS thin film, dark electrical resistance was measured in the temperature range of 333 K to 393 K. The obtained experimental data were fitted to the Arrhenius equation and a graph of conductance vs. 1000/T was plotted as shown in Fig. 7. One of

the most important electrical parameter to define is activation energy of material. Conductance increases with temperature indicating semiconducting behavior. The excitation of charge carrier from valence band to conduction band is responsible for the rise of conductivity. Activation energy was calculated from the slope of this curve and it is found to be 0.306 eV. This value is comparable to the one obtained in the previous works [3, 6]. The activation energy of SnS thin film depends on elements ratio, fabrication technique and presence of different defect states during the growth of the film [8].
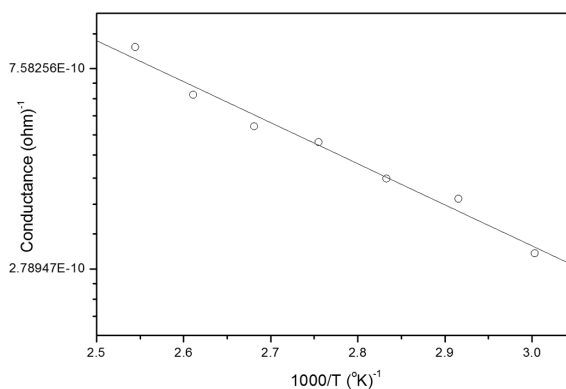

Fig. 7. Conductance vs. 1000/T graph.

Fig. 8 shows the FT-IR spectrum of SnS thin film. Strong and sharp bands appear in the spectrum at 602.48, 1094.78, 1380.64, 1630.76 and 2364.41 cm^{-1} which are due to the characteristic peaks of SnS [14, 15]. The broad band at 3421.91 cm^{-1} peak is due to O–H stretching vibrations [16–18]. The characteristic peaks of SnS in the FT-IR analysis are supported by the XRD result and they confirm the presence of SnS nanoparticles.

4.   Conclusion

SnS thin film was deposited onto glass substrate by a relatively simple method called successive ionic adsorption and reaction (SILAR). XRD study showed that the film consisted of orthorhombic phase SnS. XRD measurement showed the average particle size of ∼45 nm which has been confirmed by FESEM measurements
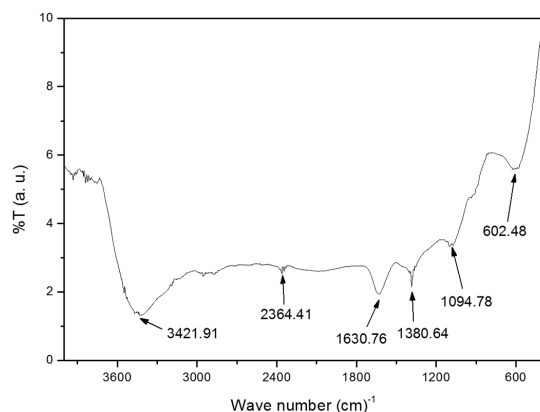
Fig. 8. FT-IR spectrum of SnS film.

using ImageJ software. The optical band gap is about 1.63 eV which is on the higher side of the bulk band gap value, possibly due to quantum confinement effect arising from reduction of particle size. Deviation of stochiometry may also have contributed to enhanced band gap. The electrical activation energy of 0.306 eV may be attributed to tin interstitials acting as donor states.

Acknowledgements

References

[1] MARIAPPAN R., RAGAVENDAR M., PONNUSWAMY V., *Opt. Appl.*, 41 (4) (2011), 989.

[2] YUE G.H., WANG W., WANG L.S., WANG X., YAN P.X., CHEN Y., PENG D.L., *J. Alloy. Compd.*, 474 (2009), 445.

[3] GUNERI E., GODE F., ULUTAS C., KIRMIZIGUL F., ALTINDEMIR G., GUMUS C., *Chalcogenide Lett.*, 7 (2010), 685.

[4] GAO C., SEHN H., SUN L., *Appl. Surf. Sci.*, 257 (2011), 6750.

[5] SOHILA S., RAJALAKSHMI M., GHOSH C., *J. Alloy. Compd.*, 509 (2011), 5843.

[6] REDDY K.T.R., REDDY N.K., MILES R.W., *Sol. Energ. Mat. Sol. C,* 90 (2006), 3041.

[7] LOFERSKI J.J., *J. Appl. Phys.*, 27 (1956), 777.

[8] PRASERT S., JAEYEONG H., WONTAE N., ADAM S.H., ROY G.G., `http://nrs.harvard.edu/urn-3:HUL.InstRepos:5366599`.

[9] SANKAPAL B.R., MANE R.S., LOKHANDE C.D., *Mater. Res. Bull.*, 35 (2000), 2027.

[10] NICOLAU Y.F., DUPUY M., BRUNEL M., *J. Electrochem. Soc.*, 137 (1990), 2915.

[11] LUTTEROTTI L., MATTHIES S., WENK H.R., *ICOTOM-12,* 1 (1999), 1599.

[12] RASBAND W.S., *ImageJ*, U.S. National Institutes of Health, Bethesda, Maryland, USA, `http://imagej.nih.gov/ij/`, 1997 – 2014.

[13] TAUC. J., *Mater. Res. Bull.*, 5 (1970), 721.

[14] HENRY J., MOHANRAJ K., KANNAN S., BARATHAN S., SIVAKUMAR G., *J. Exp. Nanosci.,* 8 (2013) 12.

[15] KHEL L.K., KHAN S., ZAMAN M.I., *J. Chem. Soc. Pak.,* 27 (2005), 24.

[16] KAMALASANAN M.N., CHANDRA S., *Thin Solid Films,* 288 (1966), 112.

[17] PAKDEL A., GHODSI F.E., *Pramana-J. Phys.,* 76 (2011), 973.

[18] XU Y., SALIM N.A., TILLEY R.D., *Nanomaterials-Basel,* 2 (2012), 54.

[19] GHOSH B., DAS M., BANERJEE P., DAS S., *Appl. Surf. Sci.* 254 (2008), 6436.